



Research article

Seismic response of RC frames equipped with buckling-restrained braces having different yielding lengths

Mohamed Meshaly^{1,2,*} and Hamdy Abou-Elfath¹

¹ Structural Engineering, Alexandria University, Alexandria, Egypt

² Construction and Building Engineering, Arab Academy for Science, Technology and Maritime Transport (AASTMT), Alexandria, Egypt

* **Correspondence:** Email: momashaly81@gmail.com; Tel: +020 1288605929.

Abstract: Buckling-restrained braces (BRBs) have proven to be a valuable earthquake resisting system. They demonstrated substantial ability in providing structures with ductility and energy dissipation. However, they are prone to exhibit large residual deformations after earthquake loading because of their low post-yield stiffnesses. In this study, the seismic response of RC frames equipped with BRBs has been investigated. The focus of this research work is on evaluating the effect of the BRB yielding-core length on both the maximum and the residual lateral deformations of the braced RC frames. This is achieved by performing inelastic static pushover and dynamic time-history analyses on three- and nine-story X-braced RC frames having yielding-core length ratios of 25%, 50%, and 75% of the total brace length. The effects of the yielding-core length on both the maximum and the residual lateral deformations of the braced RC frames have been evaluated. Also, the safety of the short-yielding-core BRBs against fracture failures has been checked. An empirical equation has been derived for estimating the critical length of the BRB yielding cores. The results indicated that the high strain hardening capability of reduced length yielding-cores improves the post-yield stiffness and consequently reduces the maximum and residual drifts of the braced RC frames.

Keywords: buckling-restrained braces; RC frames; post-yield stiffness; residual deformations; earthquake; pushover

1. Introduction

Conventional earthquake structural systems such as braced frames and moment-resisting frames are designed to withstand severe inelastic deformations when subjected to the design ground motion loading. This is because the present philosophy of seismic design depends on providing the earthquake structural systems with reliable plastic mechanisms that are capable of producing adequate inelastic lateral drifts to protect the designed buildings from collapse even under the effect of the maximum considered earthquake (MCE) loading. Consequently, a substantial amount of residual lateral deformation is expected to remain in the structure after an earthquake as a result of the large inelastic deformation demands. Large levels of residual lateral drifts in seismically designed building structures following intense ground motions can cause unsafe feelings to residents and may necessitate costly rehabilitation or even complete demolition of the structure [1,2].

Buckling-restrained braces (BRBs) are relatively new earthquake resisting structural systems that have demonstrated substantial ability in providing building structures with ductility and energy dissipation under earthquake loading conditions. The BRBs are able to achieve their full yield strength under compression axial loading because of the exterior restraining mechanism that prevents the yielding-core component from buckling. In the past few decades, extensive experimental and theoretical studies have been conducted for evaluating the BRB behavior under seismic loading [3–9].

In spite of the remarkable ductility and energy dissipation capacities of BRBs, they have a major shortcoming which is related to their low post-yield stiffness. The low post-yield stiffness of the BRBs results in large residual and maximum lateral drifts of the bracing systems under strong ground motion loading. MacRae et al. [10] reported that the low post-yield stiffness of BRBs causes a concentration of deformations in soft stories. In addition, Zaruma and Fahnestock [11] reported that the inadequate levels of post-yield stiffness of BRBs intensify the permanent deformations and increase the collapse probability under intense seismic loading.

Various techniques have been proposed to improve the BRB post-yield stiffness. This includes the use of rigid beam-column connections within the braced frame or the use of moment-resisting frames as a dual system with the braced frames [12–14]. These two techniques for enhancing the post-yield stiffness of BRBs can be used together or separately [14].

Another approach has been suggested recently for enhancing the BRB post-yield stiffness. This new approach relies on utilizing BRBs with short-length yielding-cores [15–17]. BRBs with short-length yielding-cores possess higher strain hardening capability than BRBs with long-length yielding-cores and thus reduce the maximum and residual drifts of the braced frames.

The use of BRBs for seismic strengthening of RC framed buildings has been the topic of various research studies conducted in the past two decades. The BRBs do not provide additional weight to the RC structure and can be more quickly connected to the RC structure than other strengthening procedures. Also, in the case of adding BRBs to existing RC buildings, the attachment of the BRBs to the perimeter frames can significantly reduce the construction disruptions. The previously conducted experimental and analytical studies have highlighted the efficiency of strengthening RC structures by BRBs. They also highlighted the enhancement in the overall behavior of the RC structures in terms of stiffness, strength, ductility, and energy dissipation due to the addition of the BRBs.

Mazzolani [18] conducted a full-scale experimental study on a number of modern seismic strengthening approaches including the BRBs. The results have shown the efficiency of the studied

BRBs in improving the strength, stiffness, ductility, and energy dissipation of the original RC structure. Also, Yooprasertchai and Warnitchai [19] experimentally investigated the response of BRBs connected to the RC elements by post-installed anchors. The test results confirmed the possibility of using post-installed anchors for the connection of BRBs. Moreover, the BRBs considerably improve the stiffness and strength of the RC structure and have shown to be an efficient retrofit technique for RC structures having insufficient seismic resistance.

Dinu et al. [20] conducted experimental and numerical research to evaluate the seismic behavior of RC frames strengthened by BRBs. They concluded that the strengthened structure had larger rigidity and better ductility capacity than the original RC structure. The connections between the RC elements and the BRBs acted well and the failure of the strengthened structure was because of the brace fracture in tension. Mahrenholtz et al. [21] conducted an experimental study to examine the performance of BRBs connected to RC frames by post-installed anchors under cyclic loading conditions. The results indicated that the suggested strengthening technique is capable of enhancing the strength and the ductility to a satisfactory seismic performance level.

Abou-Elfath et al. [22] studied analytically the seismic strengthening of RC frames by BRBs. They concluded that seismic upgrading of RC buildings with BRBs can considerably enhance the seismic resistance of RC structures. Their results also displayed the increase in the seismic resistance of the RC frames with the increase in the amount of the BRBs.

Ozcelik and Erdil [23] studied experimentally and numerically the seismic performance of 3-story RC frames rehabilitated with chevron BRBs by pseudo-dynamic tests. The study outcomes pointed out that seismic strengthening of RC frames by BRBs is beneficial in reducing lateral deformation and damage under earthquake loading conditions. In addition, the yielding of the BRB core plates provides the rehabilitated frames with a reliable source of energy dissipation under cyclic loading conditions.

Also, Al-Sadoon et al. [24] studied experimentally the seismic upgrading of RC framed buildings by means of BRBs. They concluded that the BRB system considerably enhanced the seismically deficient RC frames in terms of lateral strength, stiffness, and ductility. They also highlighted the enhancement in the energy dissipation due to the yielding of the BRB core plates in both tension and compression. Sutcu et al. [25] studied experimentally large-scale RC frames retrofitted with BRBs. The retrofitting scheme includes the installation of a supplementary steel frame in parallel with the BRBs. The steel frame is designed to remain elastic in order to provide the system with restoring capacity and self-centering capability. The test results pointed out that the proposed technique is capable of increasing the strength and the ductility of the RC frames to an adequate seismic performance level.

Castaldo et al. [26] evaluated the efficiency of retrofitting an existing RC building with buckling restrained braces (BRBs) employing a performance-based approach. They found that the benefit in terms of drift reduction due to the use of BRBs was evident by observing the demand hazard curves for the story drift ratios. They also concluded that the use of the BRBs results in an overall reduction of the residual story drift ratios. Xu et al. [27] and Dai et al. [28] suggested different techniques that can be used to enhance the strength and energy dissipation of RC structures. The outcomes of all the previous experimental and analytical research works reveal the effectiveness of the BRBs as a solution for enhancing the strength and energy dissipation capacities of RC structures. However, there is still a need for reducing the residual lateral deformations which are expected to remain in the structure after an earthquake as a result of the large inelastic deformation of

the BRBs. The objective of this study is to evaluate the effect of the BRB yielding-core length on the maximum and residual lateral drifts of RC frames equipped with BRBs. This is achieved by conducting inelastic static pushover and dynamic time-history analyses on three- and nine-story braced RC frames having yielding-core length ratios of 25%, 50%, and 75% of the total brace length. Also, the safety of the short-yielding-core BRBs against fracture failures due to earthquake loading has been checked by comparing their strain demands with their strain capacities determined by low cycle fatigue analysis and the AISC cyclic loading protocol.

2. Strain capacity of BRBs under cyclic loading

The strain capacity of a BRB yielding-core varies according to the cyclic loading history applied on the braces. However, it can be estimated by low-cycle fatigue analysis if the cyclic loading history is known. In this study, the strain capacity of BRB yielding-cores is estimated based on the AISC [29] loading protocol which is established for buckling restrained braced frames (BRBFs) designed according to the US standards [6]. This loading protocol has been proved by Dehghani and Tremblay [30] to be more severe than real earthquake loading conditions based on the outcomes of a considerable number of inelastic dynamic analyses conducted on 56 multi-story BRBFs. Assuming ϵ is the yielding core strain, ϵ_y is the yield strain and μ is the strain ductility ratio corresponding to the design basis earthquake loading condition (the ratio between the maximum strain divided by the yield strain). The AISC seismic provisions for steel structures require BRBs to be tested by a cyclic loading history as shown in Table 1.

Table 1. AISC Cyclic loading history for BRB.

Loading Segment	Number of Cycles	Target strain
1	2	$\pm\epsilon_y$
2	2	$\pm 0.5\mu \epsilon_y$
3	2	$\pm\mu \epsilon_y$
4	2	$\pm 1.5 \mu \epsilon_y$
5	2	$\pm 2 \mu \epsilon_y$

In this study, the well-known Coffin and Manson fracture rule is considered for estimating the strain capacity of BRB yielding cores. Razavi et al. [31] have stated that the overall fatigue life of BRBs is somehow similar for different steel grades. They also compared the outcomes of a number of Coffin-Manson equations for some previously tested specimens. They concluded that the equation derived by Nakamura et al. [32] possesses enough conservativeness for evaluating BRB fatigue capacity. This equation can be written as Eq 1:

$$\Delta\epsilon = 0.2048 N_f^{-0.49} \quad (1)$$

where, $\Delta\epsilon$ and N_f are the strain amplitude and the number of loading cycles to activate fracture of the BRB yielding core, respectively. Since the strain amplitudes of the AISC loading protocol applied on a BRB are variable, Miner's rule [33] is utilized for damage summation at the various deformation levels of the cyclic loading history as Eq 2:

$$\text{Damage index} = \sum \frac{n_i}{N_{fi}} \leq 1.0 \quad (2)$$

where n_i and N_{fi} are the numbers of cycles at each strain amplitude of the cyclic loading history shown in Figure 1 and the number of constant amplitude cycles required to trigger failure, respectively.

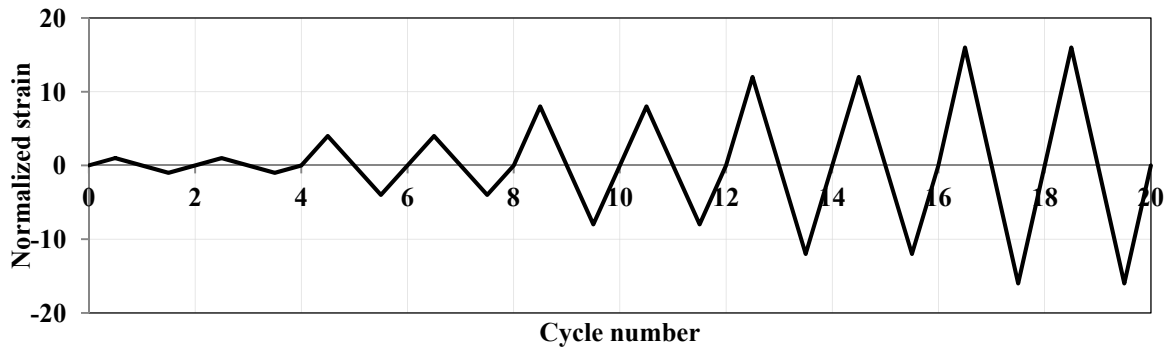


Figure 1. AISC cyclic loading protocol ($\mu = 8$).

The onset of fracture corresponds to a damage index of 1.0. The relationship between the damage index and the strain ductility ratio μ corresponding to the design basis earthquake is shown in Figure 2a, while Figure 2b represents the relationship between the damage index and the maximum strain. The maximum strain corresponds to a damage index of 1.0 is equal to 7.66%.

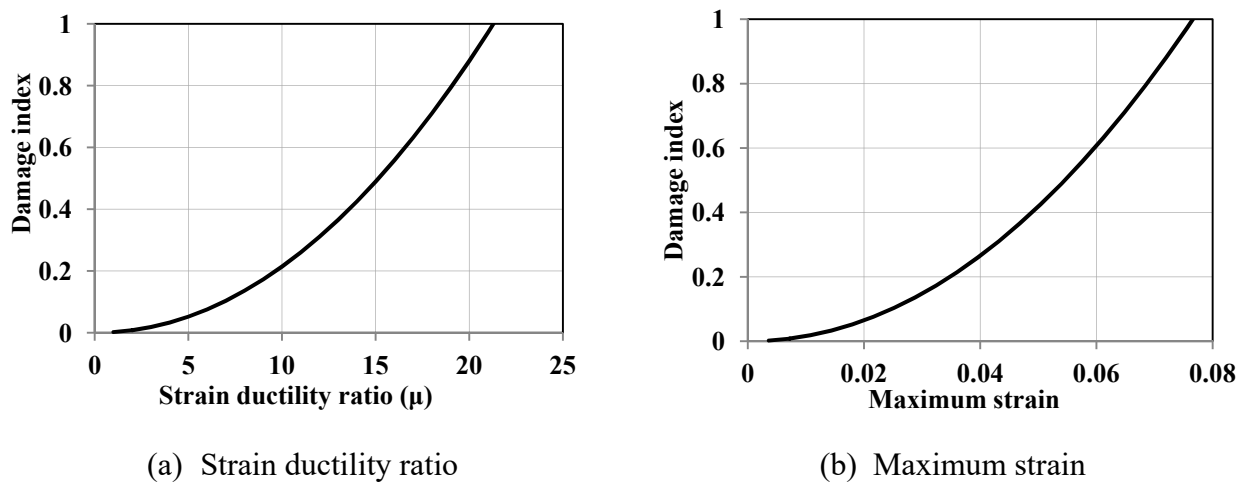


Figure 2. Low cyclic fatigue results of a BRB under the AISC loading protocol.

It should be noted that the low cycle fatigue capacity of BRBs depends on various factors other than the cyclic loading history such as the shape of the core segment, details of the restraining mechanism, eccentricity in the core segment, and the quality of manufacturing. The results of low cycle fatigue tests by Usami et al. [34] show that the existence of any discontinuities or changes in geometry can severely degrade the low cycle fatigue life of the yielding cores. Moreover, Nakamura et al. [32] have reported that the use of core cross-sections other than flat plates like cruciform

sections decreases the fatigue life property of the core element.

A number of experimental studies have reported satisfactory performance of BRBs under high strain amplitudes. Tabatabaei et al. [35] tested reduced length BRB specimens under quasi-static loading protocol and have reported that the specimens withstood high axial strains of 4–5% without any global or local failure. Pandikkadavath and Sahoo [36] tested BRB specimens under reversed cyclic loading conditions and reported that the specimens showed a stable and balanced hysteretic response up to an axial core strain of 6%.

3. The BRB minimum yielding-core length

The yielding-core strain demand level is inversely proportional to the yielding-core length. In other words, the reduced yielding-core length braces are expected to experience higher strain demands than the long yielding-core length braces. This raises concerns about the low-cycle fatigue capacity of short-length yielding cores. Determining the critical (minimum) yielding-core length requires knowing the available BRB strain capacity of ϵ_u under cyclic loading conditions as well as the story drift demands at the MCE. The Schematic illustration of lateral deformations in a braced frame is shown in Figure 3. The brace axial displacement is ΔL , the story drift is δ and the brace inclination angle is θ . The yielding-core length ratio β of the BRB is calculated in terms of the BRB strain capacity ϵ_u and the story drift demands δ as Eq 3:

$$\epsilon_u = \frac{\text{Brace axial disp}}{\beta L} = \frac{\delta \cos \theta}{\beta L}, \quad \beta = \frac{\delta \cos \theta}{L \epsilon_u} \quad (3)$$

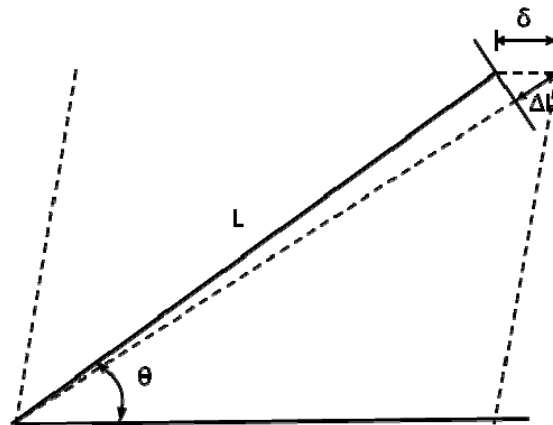


Figure 3. Schematic illustration of lateral-deformations in a braced frame.

In the current study, the peak story drift demand at the MCE is considered 4.0% based on the performance limits introduced by Fahnestock et al. [5] which are presented in Table 2. Considering a frame with a 3.6 m story height, a 6.0 m bay width, δ of 4% and ϵ_u of 0.0766 as obtained from the low cycle fatigue analysis in section 2, the critical yielding-core length ratio β can be calculated from Eq 3 as 0.23. It should be noted that the actual level of β has to be lower than the conservative estimation of Eq 3 because it ignores the elastic deformations of the transition and the connection parts at each end of the BRB.

Table 2. Response limits of steel BRB frames introduced by Fahnestock et al. [5].

Element	Limit State/Response Quantity	Design Basis Earthquake (DBE) Limit	Maximum Considered Earthquake (MCE) Limit
Brace	Core Yielding	OK	OK
	Core Fracture	No	No
	Maximum Ductility Demand	15	25
	Cumulative Ductility Demand	200	400
Drift	Maximum Roof Drift	0.015	0.03
	Maximum Story Drift	0.02	0.04

4. Materials and methods

4.1. Modelling of the braced frames

The geometry of the buckling restrained brace is shown in Figure 4. The total length of the interior steel component is L , the length of the yielding-core part is βL and the length of the transition and the connection parts at each end is $(1-\beta)L/2$. The cross-sectional area of the yielding-core is A . The average cross-sectional areas of the transition and the connection zones are assumed equal to five times the cross-sectional area of the yielding-core [37]. The modulus of elasticity, yield stress, and the strain hardening ratio of the interior steel component are denoted E , σ_y , and α , respectively. In this study, the BRB is modeled as a one-dimensional spring element with a uniaxial bilinear force-displacement kinematic hardening model. The properties of the spring model are the elastic stiffness K_1 , the inelastic stiffness K_2 , and the yield force F_y . These equivalent properties are calculated considering the varying cross-sectional area of the BRB as Eqs 4–6:

$$K_1 = 5/((1 + 4\beta)) EA/L \quad (4)$$

$$K_2 = 5/(5\beta + \alpha(1 - \beta)) \alpha EA/L \quad (5)$$

$$F_y = A\sigma_y \quad (6)$$

Table 3 summarizes the elastic and inelastic stiffness properties of BRBs in cases of β equals 25%, 50%, and 75% of the total brace length and α of 1.0%. An equivalent modulus of elasticity ($E_{\text{equ}(1)}$) for the BRB is calculated using the following Eq 7:

$$K_{\text{BRB}} = \frac{E_{\text{equ}(1)} A}{L} \quad (7)$$

where (k_{BRB}) is the equivalent stiffness of the BRB. For the post-yield data, values for the modulus of elasticity of the end zones do not reach their yielding load. The yielding core reaches its yielding load and the value of its modulus of elasticity is reduced by the strain hardening ratio. K_{BRB} and the equivalent modulus of elasticity after yield ($E_{\text{equ}(2)}$) are then recalculated. The value of the modified strain hardening can be obtained by dividing $E_{\text{equ}(2)}$ by $E_{\text{equ}(1)}$.

The RC frames are modeled using the SeismoStruct computer program [38]. The SeismoStruct is a finite element program for static and dynamic analysis of structures with considering both

material and geometric nonlinearities. The RC members are modeled using either displacement- or force-based fiber models. The RC member cross-sections are subdivided into a large number of concrete and steel fibers to capture the spread of inelasticity over the cross-sections. The concrete fibers are modeled using a uniaxial nonlinear constant confinement concrete model that follows the constitutive relationship proposed by Mander et al. [39] and the cyclic rules proposed by Martinez-Rueda and Elnashai [40]. The steel fibers are modeled using a uniaxial bilinear steel material model with kinematic hardening. The frame elements are subdivided into integration sections to capture the spread of inelasticity along the element length. In this study, beams and columns are divided into four displacement-based elements to improve the analysis accuracy. The sectional stress-strain state is obtained through the integration of the nonlinear uniaxial stress-strain response of the individual fibers forming the cross-section of the RC element. The P-delta effects are taken into account as the geometric nonlinearity is a basic property of the formulation of all the SeismoStruct elements. Centerline dimensions are considered in modeling the frames to roughly account for the flexibility of the panel zones. Every attempt to accurately model the braced RC frames has been made. However, minimal epistemic uncertainty always exists.

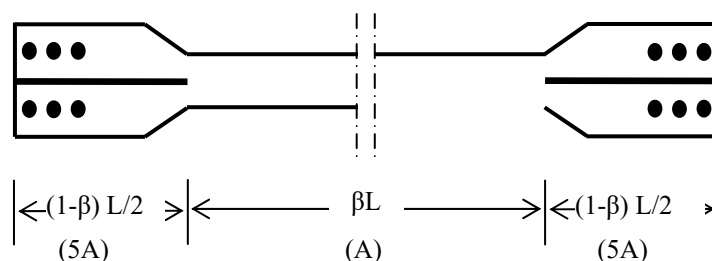


Figure 4. Geometry of the buckling restrained brace.

Table 3. Equivalent properties of the BRB spring model ($\alpha = 1.0\%$).

Core-length ratio (β)	Characterization	Equivalent axial stiffness	
		Elastic	Inelastic
75%	Long length	$K_1 = 1.25 \frac{EA}{L}$	$K_2 = 0.0133 \frac{EA}{L}$
50%	Medium length	$K_1 = 1.67 \frac{EA}{L}$	$K_2 = 0.02 \frac{EA}{L}$
25%	Short length	$K_1 = 2.5 \frac{EA}{L}$	$K_2 = 0.0398 \frac{EA}{L}$

4.2. Design of the braced frames

Three- and nine-story RC office buildings are considered in this study. The exterior frames of both buildings are assumed to be braced using an X-bracing pattern. A constant bay width of 6.0 m and a story height of 3.6 m are considered in this study. The building floorplan is shown in Figure 5 and the elevation of the exterior braced 3-story frame is displayed in Figure 6.

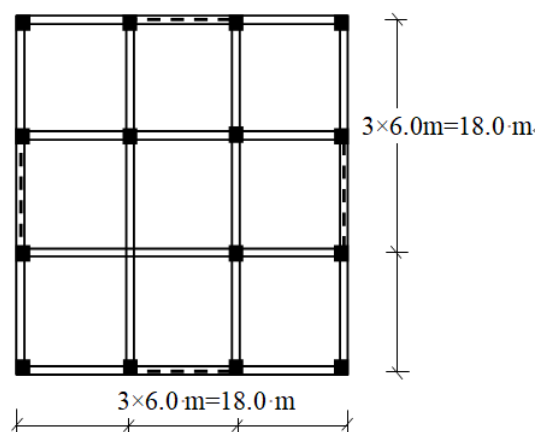


Figure 5. Floor plan of the RC buildings.

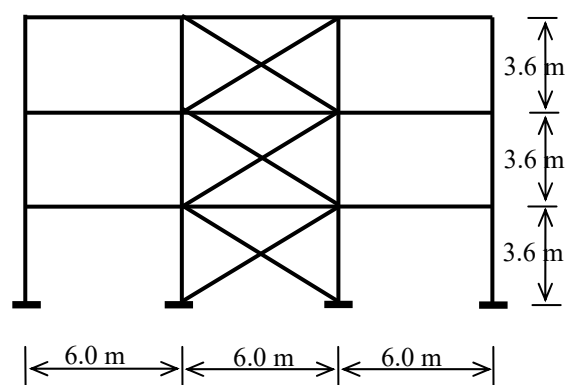


Figure 6. Elevation of the 3-story RC MRFs.

The two buildings are designed according to ACI [41] and the international building code [42]. The design spectral response acceleration parameters at short period (S_{DS}) and one second (S_{D1}) are 1.10 g and 0.59 g, respectively. A response modification factor (R), an over-strength factor (Ω_o), and deflection amplification factor (C_d) of 8, 2.5, and 5, respectively, are used. The slab thickness is 180 mm. The design dead loads included the weight of the concrete slab (4.32 kN/m^2), flooring (1.44 kN/m^2), and partition walls (0.96 kN/m^2). The design base shears are found to be 507 kN and 670 kN for the three- and nine-story frames, respectively. The frames are designed for critical combinations of dead, live, wind, and seismic loadings. Material properties for steel and concrete are summarized in Table 4.

Table 4. Material properties for steel and concrete (MPa).

Elasticity modulus of steel	200000
Brace yield stress	360
Reinforcement yield stress	413
Concrete compressive strength	27.57
Concrete tensile stress	2.75

In this study, three types of BRBs have been used for the three and nine-story RC buildings. The equivalent axial stiffnesses of the three types are calculated assuming a yielding-core length ratio of 75%, 50%, and 25%, of the total brace length. The BRB axial force is calculated from each story shear assuming that 70% of the lateral loads will be resisted by the bracing [43]. This assumption is then checked and is proved to be true. The BRB cross-sectional area is then calculated assuming a 10% strength reduction factor.

Details of the RC columns and beams are summarized in Tables 5 and 6, respectively. The column reinforcement is distributed symmetrically along the column's four sides. The steel areas of the BRBs are summarized in Table 7.

Table 5. RC column details (mm).

Frame	Stories	Exterior columns		Interior columns	
		Dimensions	Reinforcement	Dimensions	Reinforcement
3-story	1–3	300 × 300	8Ø19	400 × 400	8Ø19
9-story	1–3	450 × 450	8Ø19	500 × 500	8Ø25
	4–6	400 × 400	8Ø19	450 × 450	8Ø25
	7–9	350 × 350	8Ø19	400 × 400	8Ø25

Table 6. RC beams details (mm).

Frame	Depth	Width	Reinforcement	
			Top	Bottom
3-story	500	300	4Ø16	3Ø16
9-story	500	300	4Ø19	2Ø19

Table 7. BRB areas of the RC frames (mm²).

Story No.	3-Story	9-Story
1	639	844
2	537	836
3	325	813
4	-	772
5	-	709
6	-	623
7	-	511
8	-	371
9	-	201

4.3. Pushover analysis

The RC frames considered in this study are subjected to static lateral load having an inverted triangular distribution pattern which is a reasonable approximation for the fundamental mode response of the structure. The pushover analysis is performed before and after inserting the BRBs

into the RC bare frames. The analysis is performed using a displacement-controlled technique until reaching a 4.0% maximum story drift ratio (MSDR). The 4.0% MSDR level is considered in this study as the near-collapse limit corresponding to the MCE based on the near-collapse performance limits specified by FEMA-356 (2000) for RC frames and the MSDR demands at the MCE intensity suggested by the performance limits introduced by Fahnestock et al. [5] and were summarized in Table 1. The results of the pushover provide estimates of the structure lateral strength, lateral stiffness, and the distribution of lateral drifts along the frame heights.

4.4. Seismic analysis

The fundamental periods of the bare and the braced frames are summarized in Table 8. They have been calculated by conducting eigenvalue analysis using the SeismoStruct computer program. The fundamental periods of the braced cases are much shorter than the values of the bare frames because of the effect of the BRBs. The higher stiffness of the braced frames is expected to attract more seismic force demands. However, the higher strength capacity of the braced frames is expected to compensate for the expected rise in the seismic force demands.

Table 8. Fundamental periods of the design cases.

No. of stories	Bare frame	Braced cases		
		25%	50%	75%
3-Story	0.612	0.345	0.389	0.421
9-Story	1.458	0.881	0.965	1.026

Vamvatsikos and Cornell [44] recommended the use of 20 ground motion records from three different earthquakes (1979 Imperial Valley, 1987 Superstition Hills, and 1989 Loma Prieta) for evaluating seismic performance of low- and mid-rise buildings. The characteristics of those 20 records are summarized in Table 9. The records cover a wide range of frequency contents and durations and are utilized in the present study. This set of twenty ground motion records that belong to a bin of relatively large magnitudes of 6.5–6.9 and moderate distances, all recorded on firm soil and bearing no marks of directivity; effectively they represent a scenario earthquake. This set of nonfrequent natural records was considered to take into account the uncertainty in the seismic input [45–48].

The 3-story bare frame along with the braced cases which have BRBs with yielding-core length ratios of 25%, 50%, and 75% of the total brace length have been subjected to the suite of the twenty earthquake records. The seismic analysis is performed using Rayleigh damping which is defined to achieve 5.0% viscous damping in the first two natural modes of the structure. The seismic mass and imposed gravity loads are calculated based on the FEMA 695p [49] recommendation as 1.05 times the dead load plus 0.25 times the live load. The mass is assumed to be lumped at the beam-column joints. A time step of 0.005 seconds is used for the dynamic analysis.

The selected earthquakes are scaled to excite the structure well into the inelastic range of deformations. An MSDR of 4.0% is considered as a collapse limit for the braced frames. This MSDR limit is based on the near-collapse performance limit specified by FEMA-356 [50] for RC frames and the MSDR demands at the MCE intensity suggested by the performance limits introduced by

Fahnestock et al. [5] and were summarized in Table 1. Each earthquake record is scaled twice, one for the 3-story frame cases and one for the 9-story design cases. The earthquake scale factor is determined such that the MSDRs of braced cases have a maximum value of 4.0%. The mean PGA levels of the twenty earthquakes considered in the analysis of the 3-story and the 9-story frames are equal to 1.37 g and 1.45 g, respectively.

Table 9. Selected earthquake ground motion records.

Rec. No.	Event	Year	Record station	Φ^1	M^{*2}	R^{*3} (Km)	PGA (g)
1	Imperial	1979	Cucapah	85	6.9	23.6	0.309
2	Imperial	1979	Chihuahua	282	6.5	28.7	0.254
3	Imperial	1979	El Centro Array # 13	140	6.5	21.9	0.117
4	Imperial	1979	El Centro Array # 13	230	6.5	21.9	0.139
5	Imperial	1979	Plaster City	45	6.5	31.7	0.042
6	Imperial	1979	Plaster City	135	6.5	31.7	0.057
7	Imperial	1979	Westmoreland Fire	90	6.5	15.1	0.074
8	Imperial	1979	Westmoreland Fire	180	6.5	15.1	0.11
9	Loma Prieta	1989	Agnews State	90	6.9	28.2	0.159
10	Loma Prieta	1989	Anderson Dam	270	6.9	21.4	0.244
11	Loma Prieta	1989	Coyote Lake Dam	285	6.5	22.3	0.179
12	Loma Prieta	1989	Hollister Diff. Array	255	6.9	25.8	0.279
13	Loma Prieta	1989	Hollister Diff. Array	165	6.9	25.8	0.269
14	Loma Prieta	1989	Holister South & Pine	0	6.9	28.8	0.371
15	Loma Prieta	1989	Sunnyvale Colton Ave	270	6.9	28.8	0.207
16	Loma Prieta	1989	Sunnyvale Colton Ave	360	6.9	28.8	0.209
17	Superstition	1987	Wildlife Liquefaction	90	6.7	24.4	0.18
18	Superstition	1987	Wildlife Liquefaction	360	6.7	24.4	0.2
19	Loma Prieta	1989	WAHO	0	6.9	16.9	0.37
20	Loma Prieta	1989	WAHO	90	6.9	16.9	0.638

*Note: ¹Component, ²Moment Magnitudes, ³Closest Distances to Fault Rupture.

5. Results

5.1. Pushover results of the 3-story frames

Figure 7a,b show the base shear versus the roof drift ratio (RDR) and the MSDR of the 3-story frames, respectively. The peak base shear of the 3-story bare frame is 422 kN while that of the braced cases is 863 kN which is corresponding to the RC frame equipped with BRBs having a 25% yielding-core length ratio. The results indicate that the BRBs significantly improve the strength and the stiffness of the 3-story RC frame. The results also indicate that the frame with BRBs having a 25% yielding-core length ratio is characterized with higher strength and post-yield stiffness than the other two frames.

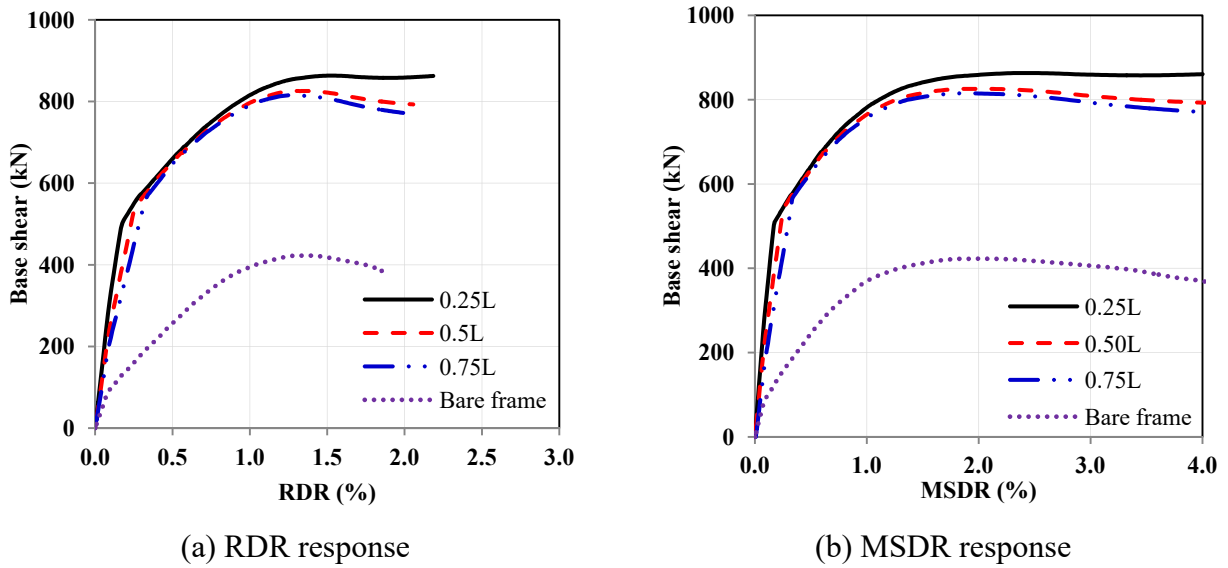


Figure 7. Pushover responses of the 3-story frames.

Figure 8a shows the height-wise distribution of the SDRs at 4.0% MSDR for the 3-story frames considered in this study. The MSDR occurs in the first story for the bare frame and the braced cases. Figure 8b shows the height-wise distribution of the strain demands in the BRB yielding cores at 4.0% MSDRs. The short-yielding-core braces experienced higher strain demands than the long-yielding-core ones as shown in Figure 8b. The peak strain demand in the BRBs with a 25% yielding-core length ratio is 7.0%. This high level of strain demand is still below the strain capacity of 7.66% calculated in section 2 in this study. The difference in strain demands between the two values is because of ignoring the elastic deformations of the BRB transition and connection parts in the derivation of Eq 3.

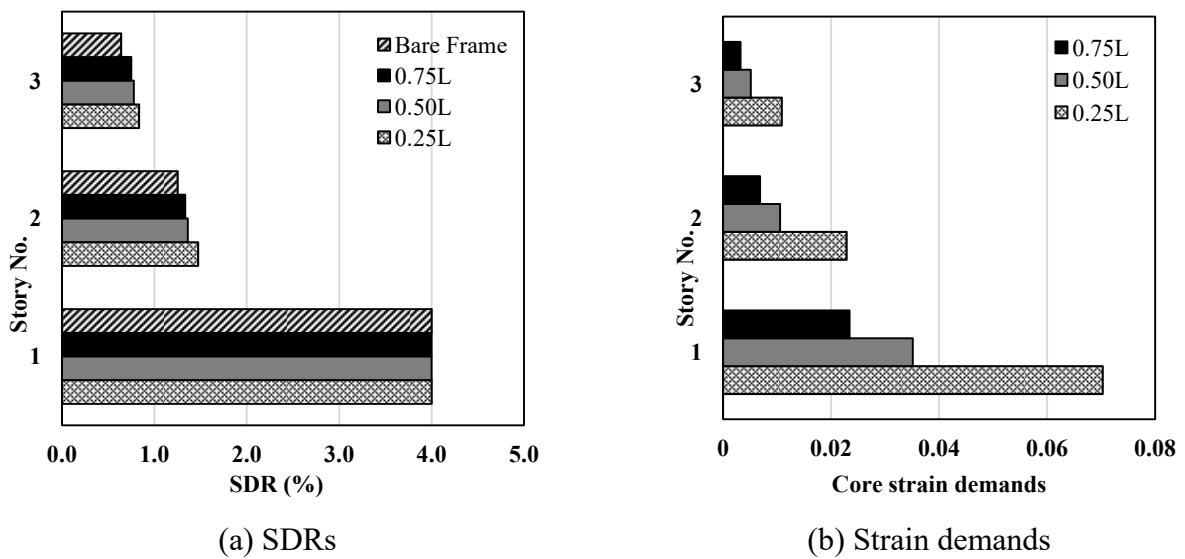


Figure 8. Height-wise distributions of the SDRs and BRB strain demands at MSDR of 4.0%.

5.2. Pushover results of the 9-story frames

The relationships between the base shear and the lateral deformations defined in terms of the RDR and the MSDR of the 9-story frames are shown in Figure 9a,b, respectively. The peak base shear of the 9-story bare frame is 602 kN while the peak base shear of the braced frame cases is 1127 kN which is corresponding to the RC frame equipped with BRBs having a 25% yielding-core length ratio. The results indicate that the BRBs significantly improve the strength and the stiffness characteristics of the 9-story RC frame. The frame with BRBs having a 25% yielding-core length ratio is characterized by higher strength and post-yield stiffness than the other two frames.

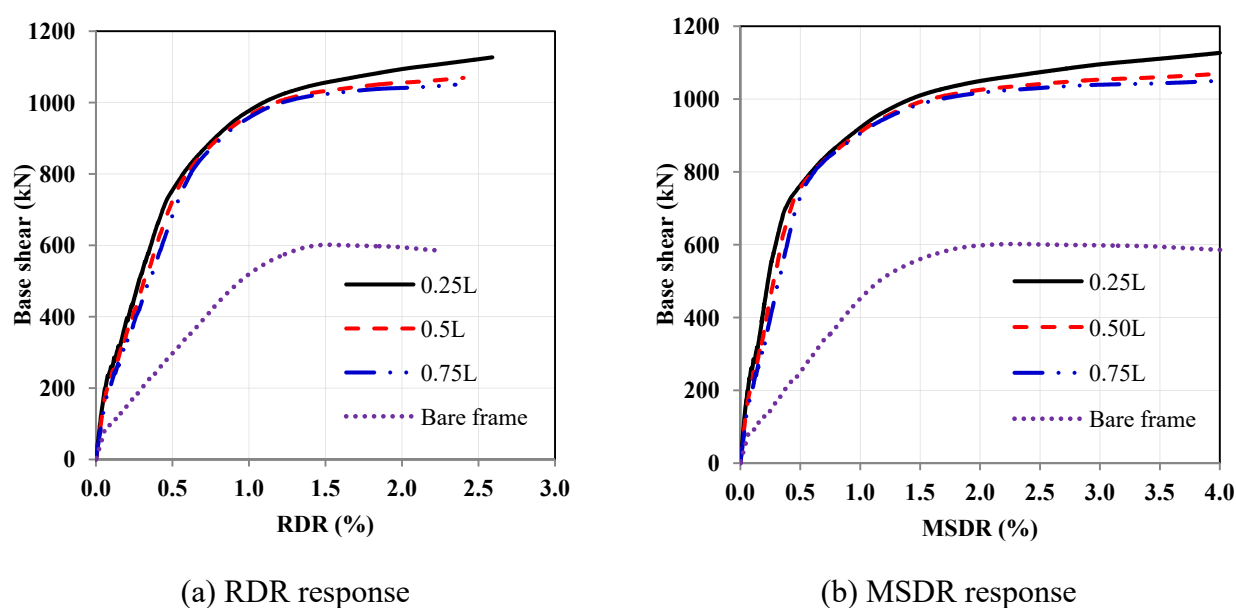


Figure 9. Pushover responses of the 9-story frames.

Figure 10a shows the height-wise distribution of the SDRs at 4.0% MSDR for the 9-story design cases considered in this study. The MSDR occurs in the second story for the 9-story bare frame and in the first story for the braced frame cases. The height-wise distribution of the strain demands in the BRB yielding-cores at 4.0% MSDRs for the 9-story design cases is shown in Figure 10b. The results of Figure 10b show that the short-length yielding-core braces experienced higher strain demands than the braces with long-length yielding-cores. The peak strain demand of the BRBs with a 25% yielding-core length ratio is 6.9%. This strain level is still below the strain capacity level of 7.66% determined in section 2 in this study. As stated before, the difference in strain demands between the two values is because of ignoring the elastic deformations of the BRB transition and connection parts in the derivation of Eq 3.

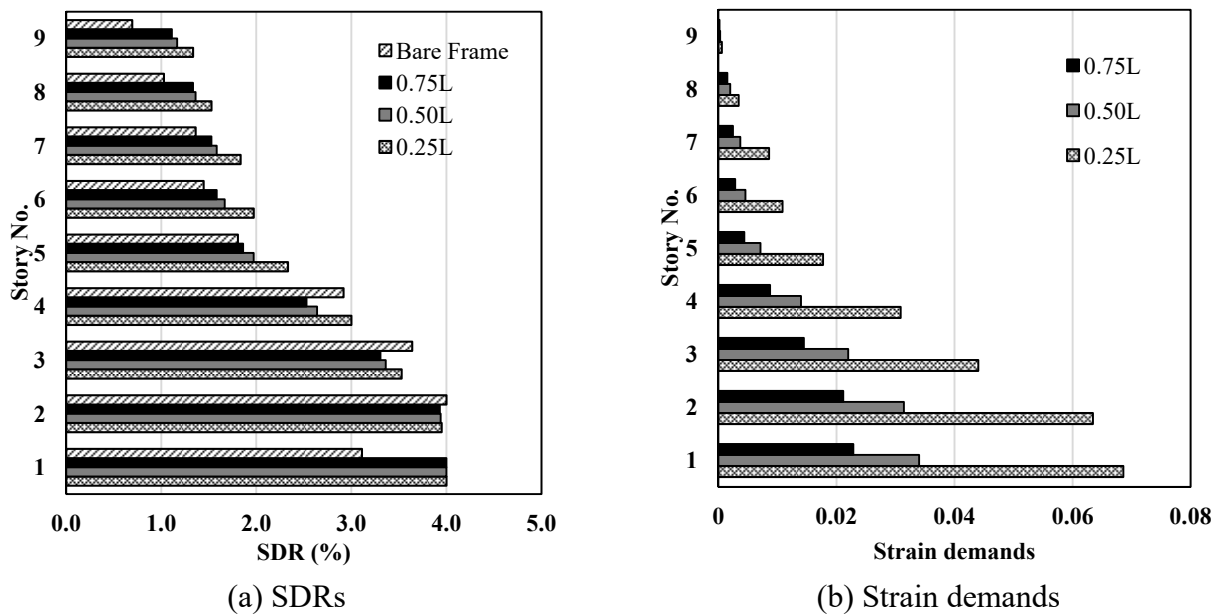


Figure 10. Height-wise distributions of the SDRs and BRB strains at MSDR of 4.0%.

5.3. Seismic performance of the 3-story frames

Figure 11a,b show the mean RDRs and MSDRs of the 3-story braced frames, respectively. The results clearly indicate a reduction in the mean RDRs and MSDRs with the reduction in the brace yielding core length. The frame designs having yielding-core length ratios of 50% and 25% exhibited mean RDRs of 8% and 15%, respectively, less than that of the frame with a yielding-core length ratio of 75%. Moreover, the frames with 50% and 25% yielding-core length ratios exhibited mean MSDRs of 8% and 17%, respectively, less than that of the frame with a yielding-core length ratio of 75%.

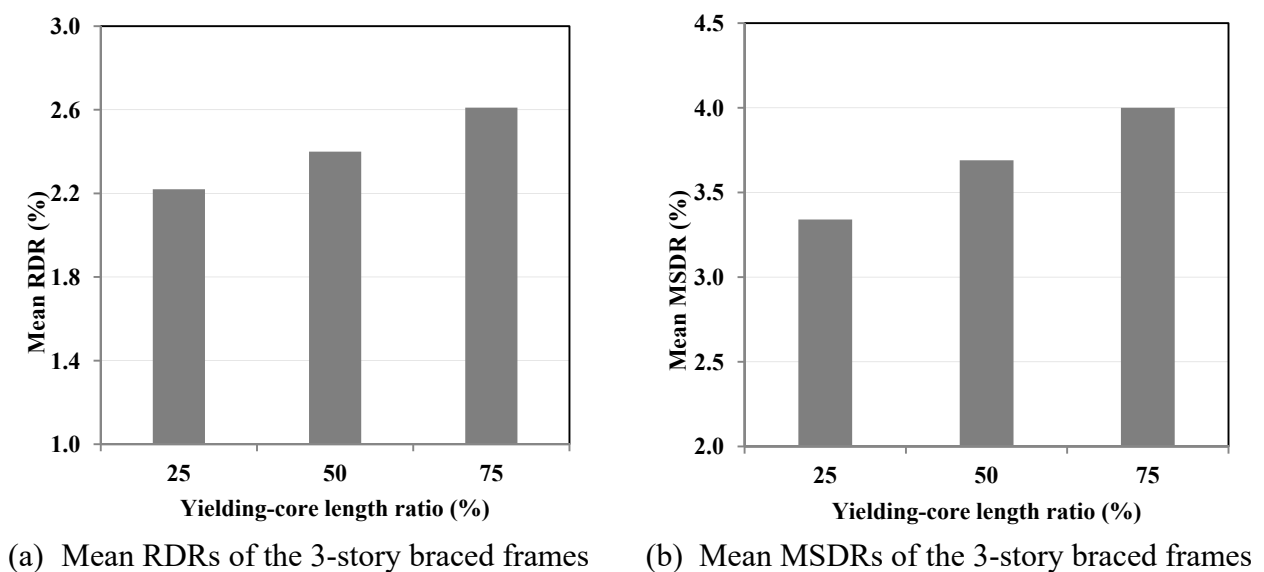
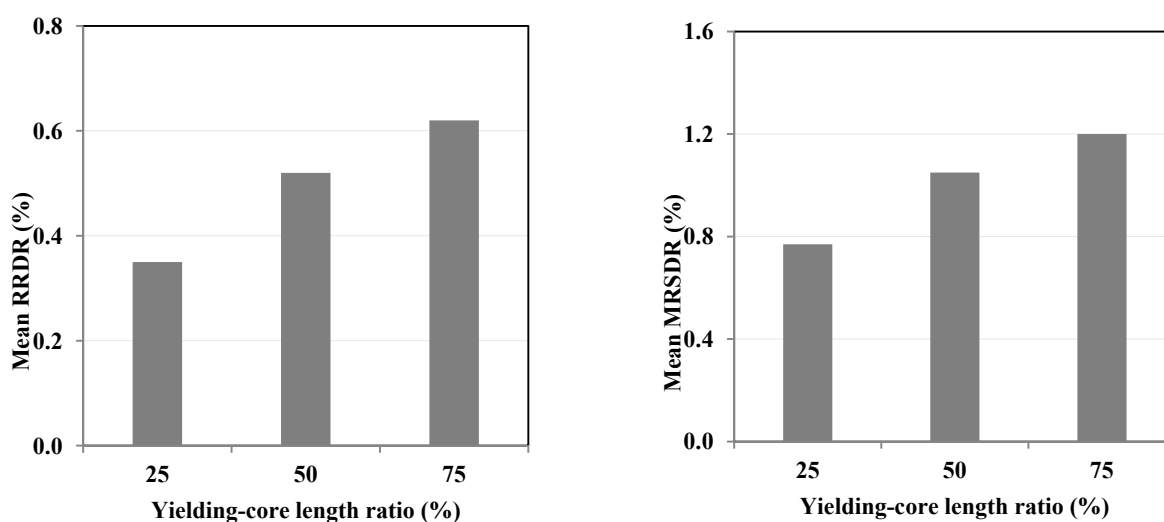


Figure 11. Mean deformation response of the 3-story braced frames.

Figure 12a,b show the mean residual roof drift ratios (RRDRs) and maximum residual story drift ratios (MRSDRs) of the 3-story braced frames, respectively. The results show a considerable reduction in the residual deformations when using BRBs with short yielding core lengths. The frame designs having yielding-core length ratios of 50% and 25% exhibited mean RRDRs of 16% and 44%, respectively, less than that of the frame with a yielding-core length ratio of 75%. Moreover, the frames with 50% and 25% yielding-core length ratios exhibited mean MRSDRs of 13% and 36%, respectively, less than that of the frame with a yielding-core length ratio of 75%.



(a) Mean RRDRs of the 3-story braced frames (b) Mean MRSDRs of the 3-story braced frames

Figure 12. Mean residual deformation response of the 3-story braced frames.

Figure 13 shows the mean strain demands of the 3-story braced frames. The results indicate that the short-yielding-core braces are expected to experience high strain demands than the long-yielding-core braces. The mean strain demand in the BRB with a 25% yielding-core length ratio is equal to 5.9% which is below the 7.0 % level reached in the pushover analysis.

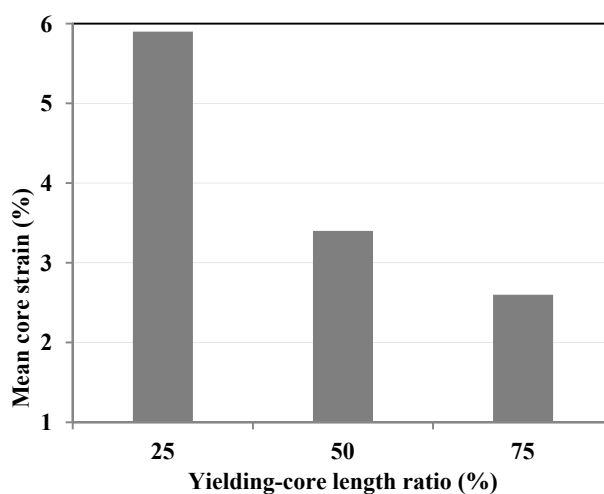


Figure 13. Mean strain demands of the 3-story frame yielding-cores.

5.4. Seismic performance of the 9-story frames

The mean RDRs and MSDRs of the nine-story frames are shown in Figure 14a,b, respectively. The results clearly indicate a slight reduction in the mean RDRs and MSDRs with the reduction in the brace yielding core length. The frame designs having yielding-core length ratios of 50% and 25% exhibited mean RDRs of 4% and 8%, respectively, less than that of the frame with a yielding-core length ratio of 75%. Moreover, the frames with 50% and 25% yielding-core length ratios demonstrated mean MSDRs of 2% and 8%, respectively, less than that of the frame with a yielding-core length ratio of 75%.

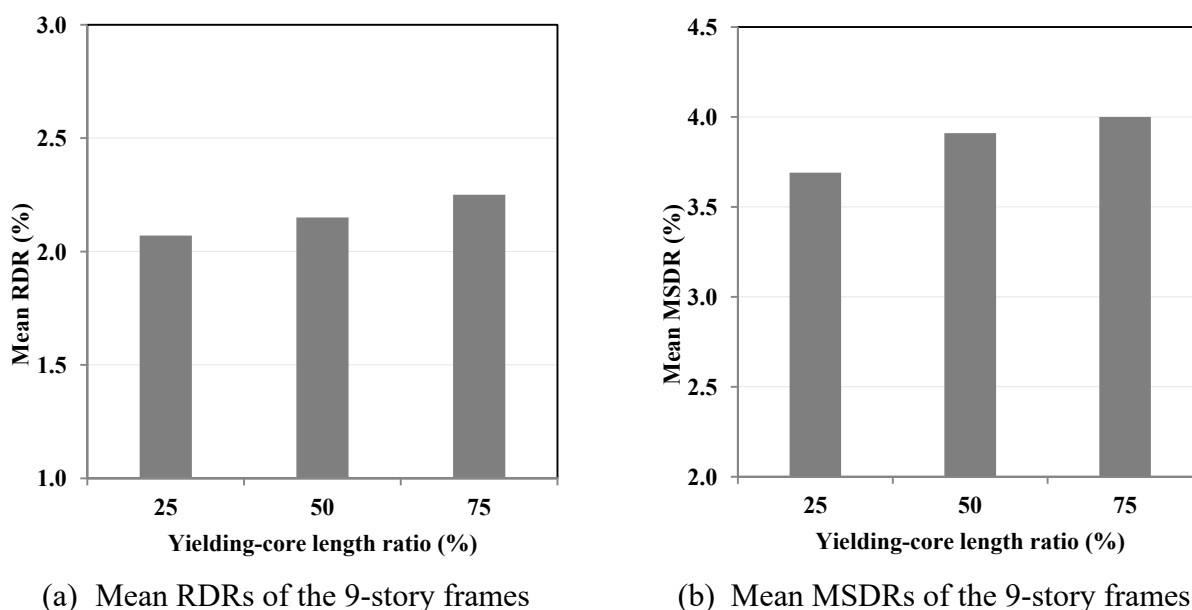


Figure 14. Mean deformation response of the 9-story frames.

Figure 15a,b show the mean RRDRs and MRSDRs of the 9-story braced frames. The results show a large reduction in the residual deformations when using BRBs with short yielding core length. The frames having yielding-core length ratios of 50% and 25% exhibited mean RRDRs of 18% and 41%, respectively, less than that of the frame with a yielding-core length ratio of 75%. Moreover, the frames with 50% and 25% yielding-core length ratios exhibited mean MRSDRs of 11% and 31%, respectively, less than that of the frame with a yielding-core length ratio of 75%.

Figure 16 shows the mean strain demands of the 9-story braced frames due to the considered earthquakes. The results indicate that the short-yielding-core braces experienced much higher strain demands than the long yielding core ones. The mean strain demand in the braces with a 25% yielding-core length ratio is equal to 5.9% which is below the 6.9% level reached in the pushover analysis.

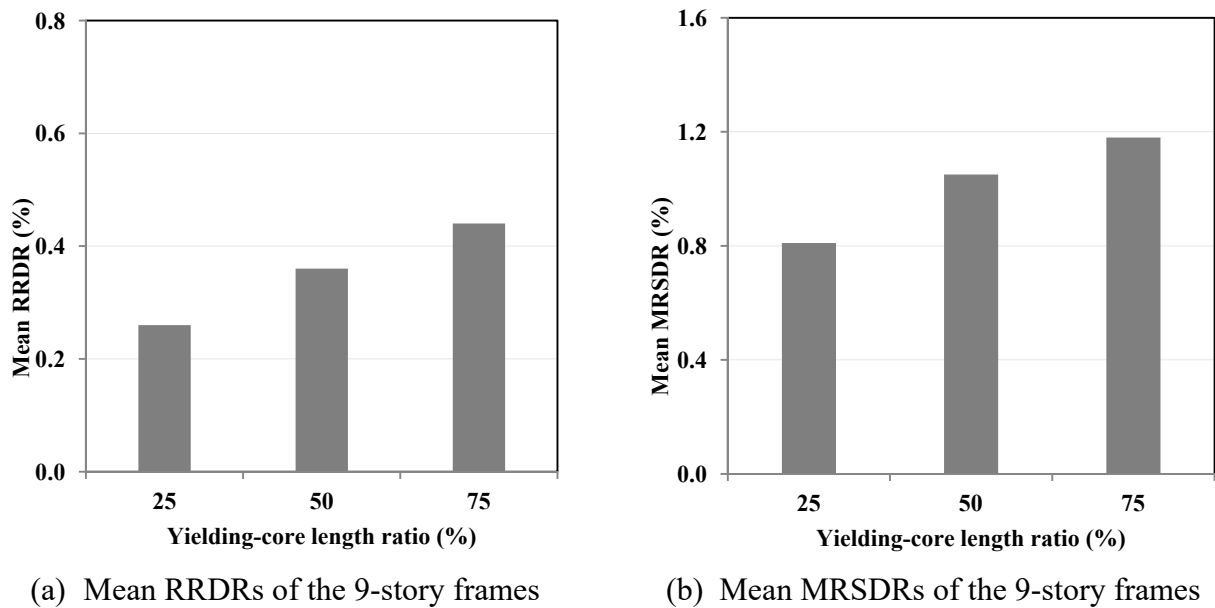


Figure 15. Mean residual deformation response of the 9-story frames.

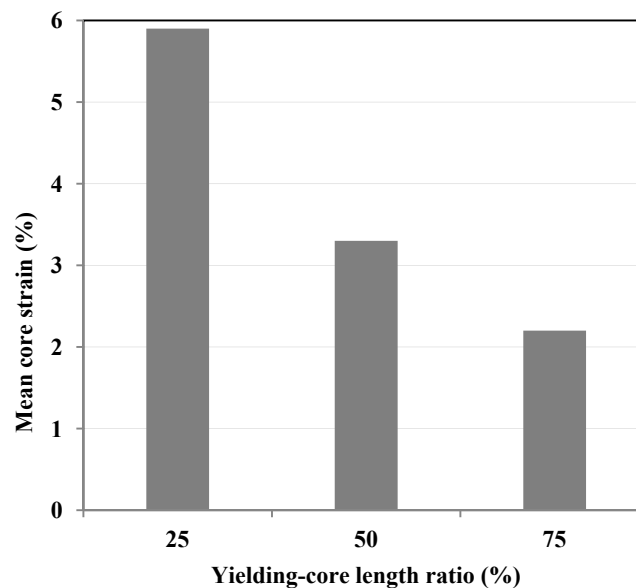


Figure 16. Mean strain demands in the yielding-cores of the 9-story braced frames.

6. Discussion

The results of the pushover analysis conducted in this study indicate that the BRBs significantly improve the strength and the stiffness characteristics of the 3-story and the 9-story RC frames. The peak strengths of the braced frames are almost double that of the corresponding bare frames. The results also indicate that RC frames with short yielding-core BRBs are characterized with higher pre- and post-yield stiffnesses than the BRBs with long yielding-core length ratios. The improvement in

the post-yield stiffnesses of frames with short yielding-core BRBs comes, unfortunately, at the expense of the high strain demands in the yielding cores of the braces. As indicated from the pushover analysis, the strain demands in BRBs with 25% yielding core length are about three times the corresponding values of the 75% yielding core length braces.

The results of the seismic analysis conducted in this study indicate that the frames with BRBs having short yielding-cores exhibited lower lateral deformation responses than those having long yielding-cores. The improvement in maximum deformation response is more pronounced in the 3-story frames than that in the 9-story frames. This indicates that the improvement in lateral deformations is not a consistent response in both the 3-story and the 9-story cases. In the 3-story frame case, the mean RDR and MSDR of the frame with BRBs having 25% yielding-core length ratio are 15% and 17%, respectively, less than that of the frame with BRBs having a yielding-core length ratio of 75%, respectively. While in the 9-story frame case, the mean RDR and MSDR of the frames with BRBs having a 25% yielding-core length ratio are only 8% less than that of the frame with BRBs having a yielding-core length ratio of 75%.

The seismic analysis results also indicate that the improvement in residual deformations is a consistent response in both the 3-story and the 9-story cases. In the 3-story frames, the mean RRDR and MRSDR of the frame with 25% yielding-core length ratio are 44% and 36%, respectively, less than that of the frame with a yielding-core length ratio of 75%. The corresponding improvements in the mean RRDR and MRSDR for the 9-story frame with 25% yielding-core length ratio are 41% and 31%, respectively, less than that of the frame with a yielding-core length ratio of 75%. These results are in agreement with Castaldo et al. [26]. The high strain hardening capacity of short-length core braces enhances the post-yield stiffness of the braced frames, thus considerably reducing the residual drift in braced RC frames under severe earthquakes.

As expected, the braced RC frames with a 25% yielding-core length ratio exhibited high strain demands in the yielding cores under severe earthquakes. As indicated from the seismic analysis, the mean strain demands in BRBs with 25% yielding core length are in the range of 6%. This high strain level can be considered acceptable and safe based on the low cycle fatigue analysis previously discussed in section 2 and on some experimental studies [16].

7. Conclusions

The effect of the yielding-core length on the maximum and residual lateral drift response of three- and nine-story braced RC frames has been evaluated in this paper. Also, the safety of the short-yielding-core BRBs against fracture failures due to earthquake loading has been checked. Based on the outcome of this study, the following conclusions can be drawn:

- The strain capacity of BRB yielding cores has been determined by low cycle fatigue analysis and by considering the AISC cyclic loading protocol and has been found to be equal to 7.66%.
- An empirical equation has been derived to estimate the critical length of the BRB yielding cores. The equation parameters are the story drift demand at the MCE, the brace inclination angle, and the BRB strain capacity. Based on this equation, the critical length ratio of the BRB yielding cores provided to the RC frames of this study is 23% of the total brace length.
- The braces with short length yielding-cores are characterized with high strain hardening capacity which generally enhances the post-yield stiffness of the braced RC frames and thus results in a considerable reduction in residual drifts. The RC frames with BRBs having a 25%

yielding-core length ratio exhibited mean RRDRs that are 41%–44% less than those of frames with BRBs having 75% yielding-core length ratio and the corresponding reduction in the mean MRSDRs ranged between 31%–36%.

- There is an improvement in the lateral deformation response of the RC frames provided with short-length BRBs. The RC frames with BRBs having a 25% yielding-core length ratio exhibited mean RDRs that are 8%–15% less than those of frames with BRBs having 75% yielding-core length ratio and the corresponding reduction in the mean MSDRs ranged between 8%–17%.
- The reduced yielding-core length braces are expected to experience higher strain demands than the long yielding core braces. The mean strain demands in BRBs with 25% yielding core length are in the range of 6% under severe earthquake loading conditions.
- More experimental work on BRBs under high strain amplitudes is still needed in order to provide more reliable data on the steel strain capacity of BRBs with short yielding-cores.

Conflict of interest

The authors declare that they have no known competing financial interests or personal relationships that could have appeared to influence the work reported in this paper.

References

1. Iwata Y, Sugimoto H, Kuwamura H (2006) Reparability limit of steel buildings based on the actual data of the Hyogoken-Nanbu earthquake, *Proceedings of the 38th Joint Panel. Wind and Seismic effects*, NIST Special Publication, 1057: 23–32.
2. McCormick J, Aburano H, Ikenaga M, et al. (2008) Permissible residual deformation levels for building structures considering both safety and human elements, *Proceedings of the 14th world conference on earthquake engineering*, China: Seismological Press Beijing, 12–17.
3. Kasai K, Fu Y, Watanabe A (1998) Passive control systems for seismic damage mitigation. *J Struct Eng* 124: 501–512. [https://doi.org/10.1061/\(ASCE\)0733-9445\(1998\)124:5\(501\)](https://doi.org/10.1061/(ASCE)0733-9445(1998)124:5(501))
4. Black CJ, Makris N, Aiken ID (2002) Component testing, stability analysis and characterization of buckling-restrained braces. PEER 2002/08, Pacific Earthquake Engineering Research Center, University of California, Berkeley.
5. Fahnestock LA, Sause R, Ricles JM, et al. (2003) Ductility demands on buckling restrained braced frames under earthquake loading. *Earthq Eng Eng Vib* 2: 255–268. <https://doi.org/10.1007/s11803-003-0009-5>
6. Sabelli R, Mahin S, Chang C (2003) Seismic demands on steel braced frame buildings with buckling-restrained braces. *Eng Struct* 25: 655–666. [https://doi.org/10.1016/S0141-0296\(02\)00175-X](https://doi.org/10.1016/S0141-0296(02)00175-X)
7. Newell J, Uang CM, Benzoni G (2006) Subassemblage testing of core brace buckling restrained braces (G Series). TR-06/01, University of California, San Diego.
8. Tremblay R, Bolduc P, Neville R, et al. (2006) Seismic testing and performance of buckling restrained bracing systems. *Can J Civil Eng* 33: 183–198. <https://doi.org/10.1139/105-103>

9. Naghavi M, Rahnavard R, Robert J (2019) Numerical evaluation of the hysteretic behavior of concentrically braced frames and buckling restrained brace frame systems. *J Build Eng* 22: 415–428. <https://doi.org/10.1016/j.jobe.2018.12.023>
10. MacRae G, Kimura Y, Roeder C (2004) Effect of column stiffness on braced frame seismic behavior. *J Struct Eng* 130: 381–391. [https://doi.org/10.1061/\(ASCE\)0733-9445\(2004\)130:3\(381\)](https://doi.org/10.1061/(ASCE)0733-9445(2004)130:3(381))
11. Zaruma S, Fahnestock LA (2018) Assessment of design parameters influencing seismic collapse performance of buckling restrained braced frames. *Soil Dyn Earthq Eng* 113: 35–46. <https://doi.org/10.1016/j.soildyn.2018.05.021>
12. Kiggins S, Uang CM (2006) Reducing residual drift of buckling-restrained braced frames as a dual system. *Eng Struct* 28: 1525–1532. <https://doi.org/10.1016/j.engstruct.2005.10.023>
13. Erochko J, Christopoulos C, Tremblay R, et al. (2011) Residual drift response of SMRFs and BRB Frames in steel buildings designed according to ASCE 7-05. *J Struct Eng* 137: 589–599. [https://doi.org/10.1061/\(ASCE\)ST.1943-541X.0000296](https://doi.org/10.1061/(ASCE)ST.1943-541X.0000296)
14. Ariyaratana CA, Fahnestock LA (2011) Evaluation of buckling-restrained braced frame seismic performance considering reserve strength. *Eng Struct* 33: 77–89. <https://doi.org/10.1016/j.engstruct.2010.09.020>
15. Hoveidae N, Tremblay R, Rafezy B, et al. (2015) Numerical investigation of seismic behavior of short-core all-steel buckling restrained braces. *J Constr Steel Res* 114: 89–99. <https://doi.org/10.1016/j.jcsr.2015.06.005>
16. Pandikkadavath M, Sahoo DR (2016) Analytical investigation on cyclic response of buckling-restrained braces with short yielding core segments. *Int J Steel Struct* 16: 1273–1285. <https://doi.org/10.1007/s13296-016-0083-y>
17. Hoveidae N, Radpour S (2021) A novel all-steel buckling restrained brace for seismic drift mitigation of steel frames. *B Earthq Eng* 19: 1537–1567. <https://doi.org/10.1007/s10518-020-01038-0>
18. Mazzolani F (2008) Innovative metal systems for seismic upgrading of RC structures. *J Constr Steel Res* 64: 882–895. <https://doi.org/10.1016/j.jcsr.2007.12.017>
19. Yooprasertchai E, Warnitchai P (2008) Seismic retrofitting of low-rise nonductile reinforced concrete buildings by buckling-restrained braces, *Proceedings of 14th World Conference on Earthquake Engineering*, Beijing.
20. Dinu F, Bordea S, Dubina D (2011) Strengthening of non-seismic reinforced concrete frames of buckling restrained steel braces, *Behaviour of Steel Structures in Seismic Areas*, 1 Ed., CRC Press.
21. Mahrenholtz C, Lin P, Wu A, et al. (2015) Retrofit of reinforced concrete frames with buckling-restrained braces. *Earthqu Eng Struct D* 44: 59–78. <https://doi.org/10.1002/eqe.2458>
22. Abou-Elfath H, Ramadan M, Alkanai FO (2017) Upgrading the seismic capacity of existing RC buildings using buckling restrained braces. *Alex Eng J* 56: 251–262. <https://doi.org/10.1016/j.aej.2016.11.018>
23. Ozcelik R, Erdil EE (2019) Pseudodynamic test of a deficient RC frame strengthened with buckling restrained braces. *Earthqu Spectra* 35: 1163–1187. <https://doi.org/10.1193/122317EQS263M>

24. Al-Sadoon ZA, Saatcioglu M, Palermo D (2020) New buckling-restrained brace for seismically deficient reinforced concrete frames. *J Struct Eng* 146: 04020082. [https://doi.org/10.1061/\(ASCE\)ST.1943-541X.0002439](https://doi.org/10.1061/(ASCE)ST.1943-541X.0002439)
25. Sutcu F, Bal A, Fujishita K, et al. (2020) Experimental and analytical studies of sub-standard RC frames retrofitted with buckling-restrained braces and steel frames. *B Earthq Eng* 18: 2389–2410. <https://doi.org/10.1007/s10518-020-00785-4>
26. Castaldo P, Tubaldi E, Selvi F, et al. (2021) Seismic performance of an existing RC structure retrofitted with buckling restrained braces. *J Build Eng* 33: 101688. <https://doi.org/10.1016/j.jobe.2020.101688>
27. Xu ZD, Shen YP, Guo YQ (2003) Semi-active control of structures incorporated with magnetorheological dampers using neural networks. *Smart Mater Struct* 12: 80–87. <https://doi.org/10.1088/0964-1726/12/1/309>
28. Dai J, Xu ZD, Gai PP, et al. (2021) Optimal design of tuned mass damper inerter with a Maxwell element for mitigating the vortex-induced vibration in bridges. *Mech Syst Signal Pr* 148: 107180. <https://doi.org/10.1016/j.ymsp.2020.107180>
29. American Institute of Steel Construction (AISC) (2016) Seismic provisions for structural steel buildings. ANSI/AISC 341-16.
30. Dehghani M, Tremblay R (2012) Development of standard dynamic loading protocol for buckling-restrained braced frames. *International Specialty Conference on Behaviour of Steel Structures in Seismic Area (STESSA 2012)*, Santiago de Chile
31. Razavi, SA, Mirghaderi, SR, Seini, A, et al. (2012) Reduced length buckling restrained brace using steel plates as restraining segment, *Proceedings of the 15th World Conference on Earthquake Engineering*, Lisbon, Portugal.
32. Nakamura H, Maeda Y, Sasaki T, et al. (2000) Fatigue properties of practical-scale unbonded braces. *Nippon Steel Tech Rep* 82: 51–57.
33. Miner MA (1945) Cumulative damage in fatigue. *J Appl Mech* 12: 159–164. <https://doi.org/10.1115/1.4009458>
34. Usami T, Wang C, Funayama J (2011) Low-cycle fatigue tests of a type of buckling restrained braces. *Procedia Eng* 14: 956–964. <https://doi.org/10.1016/j.proeng.2011.07.120>
35. Tabatabaei SAR, Mirghaderi SR, Hosseini A (2014) Experimental and numerical developing of reduced length buckling-restrained braces. *Eng Struct* 77: 143–160. <https://doi.org/10.1016/j.engstruct.2014.07.034>
36. Pandikkadavath MS, Sahoo DR (2020) Development and subassemblage cyclic testing of hybrid buckling-restrained steel braces. *Earthq Eng Eng Vib* 19: 967–983. <https://doi.org/10.1007/s11803-020-0607-5>
37. Sabelli R (2001) *Research on Improving the Design and Analysis of Earthquake-Resistant Steel Braced Frames*, California: Earthquake Engineering Research Institute.
38. SeismoStruct, 2022. A computer program for static and dynamic nonlinear analysis of framed structures. Available from: <http://www.seismosoft.com/SeismoStruct>.
39. Mander JB, Priestley MJN, Park R (1988) Theoretical stress-strain model for confined concrete. *J Struct Eng* 114: 1804–1826. [https://doi.org/10.1061/\(ASCE\)0733-9445\(1988\)114:8\(1804\)](https://doi.org/10.1061/(ASCE)0733-9445(1988)114:8(1804))
40. Martinez-Rueda JE, Elnashai AS (1997) Confined concrete model under cyclic load. *Mater Struct* 30: 139–147. <https://doi.org/10.1007/BF02486385>

41. American Concrete Institute (ACI) Committee 318 (2019) Building code requirements for structural concrete. ACI 318-19.
42. International code council (2018) *2018 International Building Code*. Available from: <https://codes.iccsafe.org/content/IBC2018/copyright>.
43. Kiggins K, Uang CM (2006) Reducing residual drift of buckling-restrained braced frames as a dual system. *Eng Struct* 28:1525–1532. <https://doi.org/10.1016/j.engstruct.2005.10.023>
44. Kiggins K and Uang CM (2006) Reducing residual drift of buckling-restrained braced frames as a dual system. *Eng Struct* 28: 1525–1532. <https://doi.org/10.1016/j.engstruct.2005.10.023>
45. Vamvatsikos D, Cornell CA (2004) Applied incremental dynamic analysis. *Earthq Spectra* 20: 523–553. <https://doi.org/10.1193/1.1737737>
46. Kitayama S, Constantinou MC (2018) Collapse performance of seismically isolated buildings designed by the procedures of ASCE/SEI 7. *Eng Struct* 164: 243–258. <https://doi.org/10.1016/j.engstruct.2018.03.008>
47. Kitayama S, Constantinou MC (2019) Probabilistic seismic performance assessment of seismically isolated buildings designed by the procedures of ASCE/SEI 7 and other enhanced criteria. *Eng Struct* 179: 566–582. <https://doi.org/10.1016/j.engstruct.2018.11.014>
48. Castaldo P, Amendola G (2021) Optimal DCFP bearing properties and seismic performance assessment in nondimensional form for isolated bridges. *Earthq Eng Struct D* 50: 2442–2461. <https://doi.org/10.1002/eqe.3454>
49. Castaldo P, Amendola G (2021) Optimal sliding friction coefficients for isolated viaducts and bridges: A comparison study. *Struct Control Hlth* e2838. <https://doi.org/10.1002/stc.2838>
50. Applied Technology Council (2009) *Quantification of Building Seismic Performance Factors*, Washington: Federal Emergency Management Agency.
51. Federal Emergency Management Agency (2000) *Prestandard and Commentary for the Seismic Rehabilitation of Buildings*, FEMA 356, Washington, DC, USA.



AIMS Press

© 2022 the Author(s), licensee AIMS Press. This is an open access article distributed under the terms of the Creative Commons Attribution License (<http://creativecommons.org/licenses/by/4.0>)